Control Engineering Practice 91 (2019) 104112

Contents lists available at ScienceDirect

Control Engineering Practice

journal homepage: www.elsevier.com/locate/conengprac

Pressure control of an electro-hydraulic actuated clutch via novel hysteresis model

Sanghun Jung [a], Seibum B. Choi [a,*], Youngho Ko [b], Jinsung Kim [b], Hoyoung Lee [b]

[a] Department of Mechanical Engineering, KAIST, 291 Daehak-ro Yuseong-gu, Daejeon, 34141, Republic of Korea
[b] Research and Development Division, Hyundai Motor Group, 150 Hyundaiyeonguso-ro, Namyang-eup, Hwaseong-si, Gyeonggi-do 18280, Republic of Korea

ARTICLE INFO

Keywords:
Hysteresis
Electro-hydraulic actuator
Pressure control
Wet clutch control

ABSTRACT

This paper mainly focuses on the development of pressure tracking control logic of electro-hydraulic actuators for vehicle application. This is done to improve and ensure the performance of a precise lower-level controller for evolving modern shift control logic. The required performance is obtained by hysteresis model-based feed-forward control and additional feedback control. The hysteresis and the time delay, which adversely affect pressure control, are well known nonlinear behaviors in electro-hydraulic actuators. In order to cope with the hysteresis, a novel hysteresis model is proposed based on a physical phenomenon. A mathematical model based on a characteristic curve obtained in preliminary experiments is presented using only one tuning parameter, and this model can be inverted easily to construct a feed-forward controller. In addition, a feedback controller is designed considering the stability margin of a time delay system. The feedback control inputs ensure compensation of the feed-forward errors caused by model error and uncertainty. The proposed controller is designed to lower computational cost considering applicability for production vehicles. As a result, the developed pressure controller is applied to a transmission control unit of a production vehicle and verified experimentally for various driving scenarios.

1. Introduction

Recently, automotive engineering technology has been studied actively from the perspective of increasing fuel efficiency. As vehicle powertrains, transmissions have a significant impact on vehicle performance and fuel efficiency. In order to achieve high fuel efficiency, modern transmission systems have been developed such as automated manual transmissions (AMTs) and dual-clutch transmissions (DCTs) (Glielmo, Iannelli, Vacca, & Vasca, 2006; Kim, Oh, & Choi, 2017; Kulkarni, Shim, & Zhang, 2007; Walker, Zhang, & Tamba, 2011). Unlike conventional automatic transmissions (ATs), AMTs and DCTs have no smoothing effect on the torque transmission since engine torque is transmitted to the clutch directly without a torque converter. Hence, these modern transmission systems require precise clutch control (van Berkel, Hofman, Serrarens, & Steinbuch, 2014; Galvagno, Velardocchia, & Vigliani, 2011). The most efficient and intuitive method of clutch control is torque-based control, because transmission systems are based on the function of torque. However, it is difficult to apply torque-based control since a production vehicle does not have a torque sensor. In order to utilize torque-based control in production vehicles, many studies on the design of a driveline torque observers and observer-based controllers have been conducted. Kim, Oh, and Choi (2018) and Oh and Choi (2015). In general shifting situations, clutch torque can be modeled to be proportional to the clutch engagement force. Therefore, precise control of the clutch actuator is an important issue for accurate torque-based shift control (Vasca, Iannelli, Senatore, & Reale, 2011).

Both hydraulic actuators and electro-mechanical actuators are used widely as actuators for clutch engagement. The electro-mechanical actuator transmits the clutch engaging force using a mechanical gear system. Since the gear is directly engaged, nonlinearity and uncertainty caused by the actuators are negligible. For hydraulic actuators, an electro hydraulic valve (EHV) based on a proportional solenoid valve (PSV) is widely used (Balau, Caruntu, & Lazar, 2011). PSVs have the advantage of high power-to-weight ratio and easy implementation of proportional control of pressure or flow rate in hydraulic systems. Due to these characteristics of PSVs, EHV actuators are widely applied to many production vehicles as actuators for clutch pressure control.

Unlike electro-mechanical actuators, EHV system is known to have its own nonlinear elements such as hysteresis, time delay, fill phase dynamics, and other uncertainties (Fu, Liu, Cui, & Xu, 2016). These nonlinear factors affect the performance of pressure tracking control negatively. In general, clutch applied force is proportional to the clutch chamber pressure. Therefore, torque-based control requires precise pressure tracking control. For this reason, several studies have been

* Corresponding author.
E-mail address: sbchoi@kaist.ac.kr (S.B. Choi).

https://doi.org/10.1016/j.conengprac.2019.104112
Received 30 January 2019; Received in revised form 30 May 2019; Accepted 7 August 2019
Available online xxxx
0967-0661/

conducted recently to improve the control performance of pressure. In Walker, Zhu, and Zhang (2014), the authors developed precise mathematical modeling for analysis and control of the hydraulic actuator system. In Guo, Liu, Zhang, and Xu (2014), Montanari, Ronchi, Rossi, Tilli, and Tonielli (2004) and Song, Zulkefli, and Sun (2010), the authors designed a model-based EHV controller based on a mathematical model. However, most studies have focused on control of the clutch filling process in the low-pressure range to improve the ride quality and response time. In addition to the fill phase, hysteresis is also an important nonlinear component of EHV system. Nevertheless, study of hysteresis compensation has not been considered as equally important. In systems with hysteresis, hysteresis compensation control is essential for accurate tracking control. Therefore, EHV hysteresis compensation is essential for the tracking control of desired torque, which varies depending on the shifting conditions.

Modeling of and compensation of hysteresis has been studied widely in various fields. The most widely used hysteresis compensation method is to apply feed-forward control constructed using identified hysteresis curves (Eielsen, Gravdahl, & Pettersen, 2012; Ru, Chen, Shao, Rong, & Sun, 2009; Ryba, Dokoupil, Voda, & Besançon, 2017). It is well known that using feed-forward control improves tracking performance generally without stability issues compared to using general feedback control. Several studies were conducted on precise modeling of hysteresis to improve the accuracy of feed-forward control. Many novel methods of modeling hysteresis curve were proposed in Choudhury, Thornhill, and Shah (2005) and Sheng, Hai, Cheng, and Bao-Lin (2013). A major shortcoming of previous research is the lack of responsiveness to dynamic situations. In fact, hysteresis curves represent a steady-state characteristic. A controller designed with a steady-state value can cause chattering or instability in dynamic situations. In order to solve the problem of discontinuity caused by this static model, novel dynamic models of hysteresis were established using various friction models such as Dahl, Lugre, Coulomb models, among others (Naser & Ikhouane, 2015; Xu & Li, 2010). However, these models are based on a differential of input and output variables; they are not simple enough to apply in practical application. In addition, since hysteresis characteristics are different for each plant, it is difficult to apply these models as a general solution.

Hence, using feed-forward control, this paper focuses on developing a simple but precise model of hysteresis to improve the control performance of an EHV system. The proposed hysteresis model is designed as a continuous, asymptotic function using a single tuning parameter to reflect the plant characteristics and actual dynamic behavior. Feed-forward controller using the hysteresis model copes better with dynamic situation than do previous methods. In order to improve the robustness of the pressure control, the feedback controller is designed with a consideration of the time delay of EHV system. Feedback controller plays a role in responding to model error and uncertainty. This paper contributes to achieving precise pressure tracking control performance of EHVs in production vehicles using the proposed control system.

The rest of the paper is organized as follows. In Section 2, the mathematical model of hysteresis is introduced and analyzed. In Section 3, pressure controller based on the proposed hysteresis model is designed. Simulation results and experimental validation in real vehicle test are presented in Section 4 and conclusion is provided in Section 5.

2. System and modeling

2.1. System description

General configuration of EHV actuator in drivetrain system is illustrated in Fig. 1. EHV actuator system consists of PSV and clutch chamber. When command current is applied to the solenoid, a magnetic force is generated. Through its own feedback structure, PSV generates output pressure proportional to the magnetic force. The output pressure

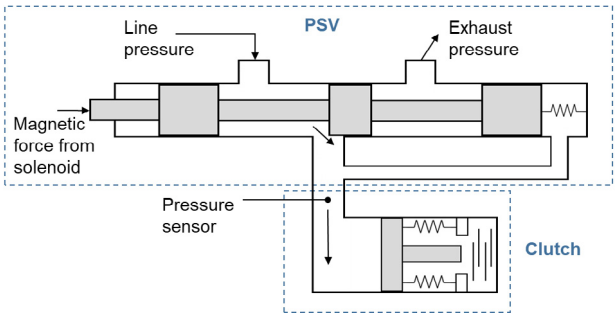

Fig. 1. Schematic of electro-hydraulic valve actuator.

generated by the PSV pressurizes the clutch chamber to actuate the clutch engagement. Therefore, pressure of clutch chamber can be controlled proportionally through current input. As a result, the input and output of the target system are the command current and the measured pressure, respectively. In order to apply precise feed-forward control, the relationship between input current and output pressure must be accurately determined. As Fig. 1 illustrates, targeted EHV system has pressure sensor to measure clutch chamber pressure. Measured pressure data are used for I–P relationship analysis and controller design.

In Guo et al. (2014), Montanari et al. (2004) and Walker et al. (2014), detailed modeling of EHV system was conducted. Authors analyzed and constructed mathematical models considering spool dynamics and clutch filling phase caused by clutch piston motion. Because of spool, clutch, and pressure dynamics, a complex model is used to describe EHV behavior . However, this paper focuses on input–output hysteresis rather than on internal dynamics of EHV system. Thus, several assumptions are made to ignore the internal dynamics. First, the PSV system is treated as a static system because the bandwidth of the PSV is much larger than the control bandwidth. Second, nonlinear effects caused by PSV, such as stiction or dead-band effects, are negligible. Finally, nonlinearity of filling phase is assumed to be compensated using previous studied methods, i.e., filling phase is not considered in this study. Under the above assumptions, the relationship between the I and P is analyzed.

In EHV system, hysteresis loops commonly appear because of energy dissipation from the solenoid and hydraulic friction loss. Experiments for measuring pressure and current were conducted with a triangular wave sweeping scenario. Experimental results that illustrate the system input–output hysteresis are shown in Figs. 2a and 2b show time domain data of input and output signals. Fig. 2a shows the hysteresis loops in the I–P domain; these indicate the steady-state characteristic of EHV. As can be seen in the graph, in the steady state, the output pressure indicates the value of the ascending/descending curve according to the sign of the input gradient. Therefore, it is easy to model the I–P relationship by identifying the ascending/descending curves in steady-state situation. However, in transient state in which the sign of the input gradient changes, the output pressure is indicated by the value between the ascending/descending curve, as shown in the zoom plot in Fig. 2c. In addition, since the behavior of the actual system contains information about the physical state of the previous situation, the output value is affected by the previous behavior of the system. For example, when the input tends to increase, the output value is found near the ascending curve value. On the other hand, when the input tends to decrease, the output value is found near the descending curve value. These physical phenomena generate hysteresis loops.

In fact, in real vehicle shift control, desired pressure can oscillate depending on the torque control strategy or the slip control strategy. It is not easy to represent an oscillated input using only a steady-state map. Therefore, in order to track the target pressure accurately, a precise prediction of the relationship between I and P in a dynamic situation is needed.

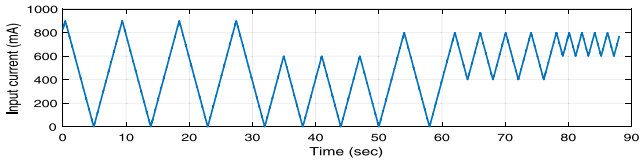

(a) Input trajectory : current

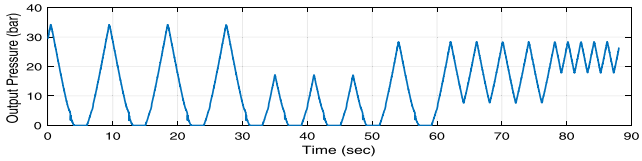

(b) Output pressure

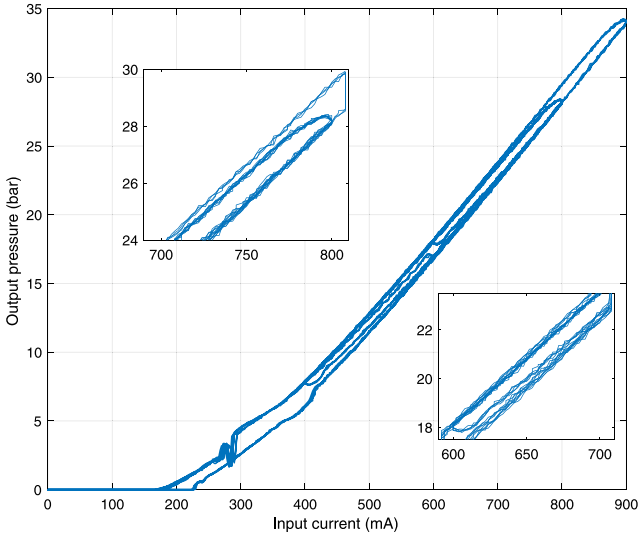

(c) Current-Pressure relationship

Fig. 2. Experiment results in respect of EHV hysteresis.

EHV system is well known to have not only hysteresis but also time delay between input and output (Balau et al., 2011). In EHV systems, output pressure is generated according to an input command with a pure time delay T_d. This time delay is the actuation delay, which makes it difficult to control the undeterministic reference input. The output of the actuation delay system is generated according to the following equation:

$$P_m(t) = P_d(t - T_d) \tag{1}$$

where $P_m(t)$, and $P_d(t)$ indicates the measured output pressure and desired reference pressure, respectively. In this paper, the time delay T_d is assumed to be a fixed and known value from the previous experiments. These physical phenomena of EHV system will be considered in the design of the controller in Section 3.

2.2. Hysteresis modeling

Here, the mathematical model for hysteresis of EHV system is introduced. In order to reflect the physical phenomena of hysteresis, the model must satisfy the following conditions:

C1. The model must be a continuous, convergent function with a steady-state curve(point).
C2. The model must reflect the past information to generate the current value.
C3. For input $u(t)$ and output $y(t)$, the model must satisfy following equation : $\frac{du(t)}{dt} \cdot \frac{dy(t)}{dt} \geq 0 \ \forall t \geq 0$

It is obvious that C1 and C2 are conditions of a general hysteresis model (Choi, Won, Lee, & Park, 2017). C3 indicates the relationship between input and output. C3 means that if the input is increased/decreased, the output must also increase/decrease, respectively. These are obvious conditions for a single-input single-output system, such as EHV system.

The first step in hysteresis modeling is to identify a reference hysteresis curve that represent the steady-state characteristic. When the reference curves have the form shown in (2), the following assumptions for reference curves are made to establish the hysteresis model.

$$f_{ref}(u) = \begin{cases} f_{ascend}(u) & \text{if } \frac{du}{dt} > 0 \\ f_{descend}(u) & \text{if } \frac{du}{dt} > 0 \end{cases} \quad \text{for input } u \tag{2}$$

A1. $f_{descend}(u) - f_{ascend}(u) > 0$, for $u_{min} < u < u_{max}$
A2. $f_{ref}(u)$ is continuous and monotonically increases with respect to u, i.e. $\frac{df_{ref}(u)}{dt} \geq 0$

A1 means that ascending and descending curves do not cross each other in the hysteresis loop within the input range. Some hysteresis characteristics show $f_{ascescend}(u_{max}) = f_{descend}(u_{max})$, but satisfy A1 within the control range. Also, A2 describes the input and output relationship. In general, a steady state curve does not decrease while input is increasing. These phenomena are general characteristics of hysteresis so that most hysteresis situations satisfy the above assumptions. The hysteresis model proposed in this paper is based on the above assumptions.

In the hysteresis of the targeted EHV, the output pressure converges to its steady-state curve depending on the sign of the input gradient, as shown in Fig. 2. Therefore, reference curves should be identified from steady-state experimental results. The experimental data were obtained using triangular inputs with a period of 40 s and the corresponding outputs. Since the scenario is sufficiently slow, the results can be thought of as having a steady-state characteristic. The reference curves are identified as 3rd order polynomial ascending/descending curves. The coefficients of the polynomial are identified using the Least-Mean-Square method. The obtained reference curves are expressed as the following equations:

$$f_{ref}(i) = \begin{cases} f_{ascend}(i) = -42.65i^3 + 92.5i^2 - 8.4i - 2.03 & \text{if } \frac{du}{dt} > 0 \\ f_{descend}(i) = -40.01i^3 + 83.32i^2 - 1.3i - 2.41 & \text{if } \frac{du}{dt} > 0 \end{cases} \tag{3}$$

where i denotes the input command in units of amperes. Fig. 3 shows the results of 3rd order polynomial curve fitting. Both ascending and descending curves are fitted with high accuracy ($R^2 = 0.99$ in both curves). As shown in Eq. (3) and Fig. 3, reference curves monotonically increase within the control range; i.e. $\frac{df(i)}{dt} \geq 0$ for $0 < i < 1$. It is clear that this satisfies the assumptions A1 and A2. These curves can be obtained when the vehicle is first started, so the curve values can be treated as known values.

In this paper, the hyperbolic function is proposed as a hysteresis model that reflects the above phenomena. The hyperbolic function is well known to have two asymptotes. The simplest hyperbolic function, $y = -1/x$, is a function with $x = 0$ and $y = 0$ as asymptotes. This function can be transformed to have oblique asymptotes through an axis transformation, as follows:

$$y - y_0 = -\frac{a}{g(x) - y} \tag{4}$$

Eq. (4) is the function with $y = y_0$ and $y = g(x)$ as asymptotes. The constant a indicates the degree of asymptotics. For smaller values of a, the function converges to its asymptotes more rapidly. In addition, a function of form (4) has a characteristic that generates two y values for a specific x value. A function with these characteristics can be applied to the current–pressure relationship, which is the target system.

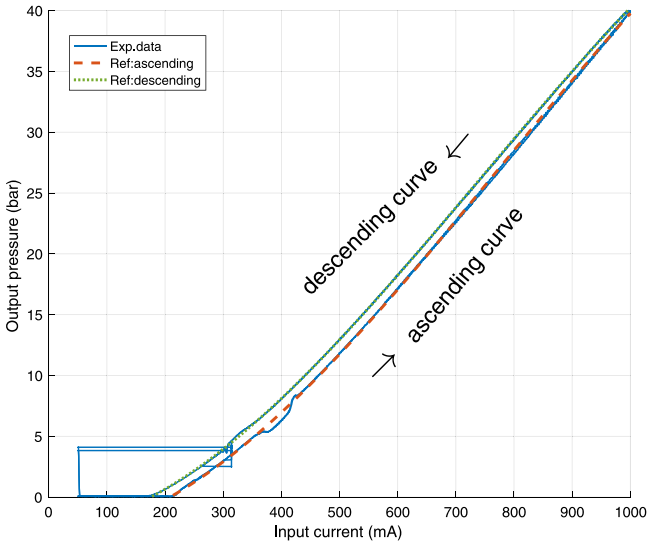

Fig. 3. Curve fitting of reference curve.

As mentioned above, according to the sign of the input gradient, EHV system converges to a reference curve in steady state, and has a value between curves in transient state. Thus, the relationship between the input current and the output pressure can be expressed as (5).

$$P(i) = -\frac{a}{f_{ref}(i) - P(i)} + P_t \tag{5}$$

Here, $f_{ref}(i)$ refers to the (3) and P_t is a constant to be calculated later. Similar to (4), Eq. (5) is a function that converges to $f_{ref}(i)$ and P_t according to the state of input i. Fig. 4 shows the graphs of (5) for arbitrary constant P_t. Increasing/decreasing situations are illustrated in Figs. 4a and 4b, respectively. As mentioned before, there are two solutions for specific i in (5). These two solutions are denoted as P_u and P_d in Fig. 4. P_u represents the larger value, and P_d represents the smaller value of the two solutions. In a real plant, the trajectory of the pressure converges on an ascending curve while increasing, and follows a descending curve while decreasing. Therefore, P_u and P_d become the unique solution of (5) in increasing and decreasing states, respectively. By specifying the unique solution, (5) becomes a single input-single output function. It can be confirmed that (5) satisfy the first condition of hysteresis model, C1, because it is continuous single-input single-output function. Since function $P(i)$ is a function of $f_{ref}(i)$, which varies with input state, function $P(i)$ must be updated at every step. In order to analyze $P(i)$ at an arbitrary step, the discrete form of (5) is expressed as follows:

$$P_k = -\frac{a}{f_{ref}(i_k) - P_k} + P_{t,k} \quad (k = 0, 1, 2, \ldots) \tag{6}$$

where P_k, i_k and $P_{t,k}$ represent the kth step of the model value, input i and the constant P_t, respectively. In order to complete the model, the constant P_t should be specified. The first condition for the hysteresis model, C1, was about continuity. If the function of the current step contains the value of the previous step, i.e. the function P_k contains (P_{k-1}, i_{k-1}), then this model can be said to be continuous. Thus, Eq. (7) is established by substituting (P_{k-1}, i_{k-1}) in (6) and rearranging it.

$$P_{t,k} = P_{k-1} + \frac{a}{f_{ref}(i_{k-1}) - P_{k-1}} \tag{7}$$

$$P_k = \begin{cases} \frac{1}{2}(P_{t,k} + f_{ascend}(i_k)) \\ \quad + \sqrt{(P_{t,k} + f_{ascend}(i_k))^2 - 4(P_{t,k} f_{ascend}(i_k) - a)} & \text{if } i_k > i_{k-1} \\ \frac{1}{2}(P_{t,k} + f_{descend}(i_k)) \\ \quad - \sqrt{(P_{t,k} + f_{descend}(i_k))^2 - 4(P_{t,k} f_{descend}(i_k) - a)} & \text{if } i_k < i_{k-1} \\ P_{k-1} & \text{if } i_k = i_{k-1} \end{cases} \tag{8}$$

The values in the previous step (P_{k-1}, i_{k-1}) are known and can be treated as constants. Since the terms on the right-hand side of (7) are all predetermined values, the constant $P_{t,l}$ can be calculated directly. The final goal of the model is to calculate the output pressure with input command i. Model (6) has the form of an implicit function. Solving this function explicitly leads to the final model Eq. (8).

Model (8) calculates P_u in increasing state and P_d in decreasing state for arbitrary input i, as described above. Thus, it is clear that model (8) becomes a single input single output function according to the input state. In addition, the model value of current state P_k is the function of input command i_k and previous state (P_{k-1}, i_{k-1}). Since the model value P_k is updated at every step and is calculated using the previous step value, it reflects the past information recursively. This means the model (8) satisfies the second condition for hysteresis model, C2. This condition is experimentally verified later.

The satisfaction of the equation third condition for hysteresis model, C3, can be confirmed by comparing the input and output gradients. Applying C3 to the target EHV system, it can be represented by $\frac{di}{dt} \cdot \frac{dP}{dt} > 0$, which is equivalent to $\frac{dP}{di}$. The derivative of model (5) with respect to input i yields to the following equation.

$$\frac{dP(i)}{dt} = \frac{a}{(f_{ref}(i) - P(i))^2} \cdot \frac{df_{ref}(i)}{dt} \tag{9}$$

The reference curve $f_{ref}(i)$, which is described in (3), is a monotonically increasing function, i.e. $\frac{df(i)}{di} > 0$. Therefore, $\frac{dP(i)}{di} > 0$ is always a positive value for a non-negative constant a. This is an obvious result because the model is designed to converge to a monotonically

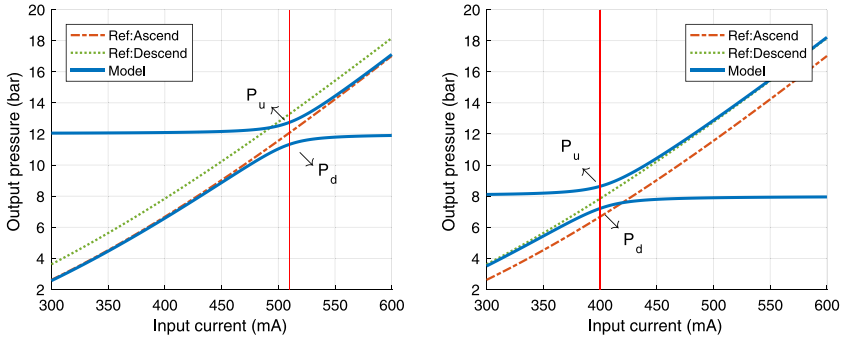

(a) Ascending case (b) Descending case

Fig. 4. Concept illustration of proposed hysteresis model.

increasing reference curve. As a result, the proposed hysteresis model meets conditions C1, C2, and C3.

The important feature of the model is that the inverse model can be calculated analytically. Since the final goal of modeling the hysteresis is to calculate the feed-forward input, the possibility of inverse model computation is important. Another main advantage of the hyperbolic model is that the model has only one tuning parameter, a. Many previously proposed hysteresis models (Eielsen et al., 2012; Ryba et al., 2017) required many tuning parameters. The most famous hysteresis model, the Prandtl–Ishlinskii operator (Al Janaideh, Rakheja, & Su, 2011), also had the advantage of making it easy to obtain an analytical solution of the inverse model, but it had a disadvantage in that it is difficult to tune many weighting factors of the model. On the other hand, the proposed model uses the pre-determined reference curves and a unique tuning parameter to reflect the hysteresis phenomenon. In addition, the model is composed of a single form of function rather than a transition of functions according to state. This makes the model output much smoother and more realistic. This also makes it easy to analyze the characteristics of the model, as in Eq. (9). Also, the proposed model generates output by mapping the input to a simple function, so that the output does not have phase distortion regardless of input of various frequencies. This leads to improvement of model accuracy for high frequency inputs.

2.3. Model validation

To verify the accuracy of the proposed hysteresis model, experiments on EHVs in production vehicles were carried out. Detailed description of the experimental environment is provided in Section 4. Since the main purpose of this section is to evaluate the accuracy of the model, actual output values and model values for the same inputs are compared. The model values are generated considering the actuation delay described in (1).

A triangle sweep with a various amplitude input profile was designed as shown in Fig. 5a. The following experimental and hysteresis model responses are depicted in 5b. In the hysteresis model, the tuning parameter a is set to 1. The root-mean-square error (RMSE) between the actual and model value is 0.173 bar. The hysteresis model works well not only for a monotonous state, but also for a direction-changed state. The I–P domain graph shows the similarity between actual and model response. Therefore, it can be seen that the proposed model represents the actual hysteresis loop and its phenomena well.

In many production vehicles, EHV hysteresis phenomenon is calculated using the average value of the ascending and descending curves, which is described as P_{ave}.

$$P_{ave}(i) = \frac{1}{2}(f_{ascend}(i) + f_{descend}(i)) \tag{10}$$

In order to demonstrate the effectiveness of the proposed model, results of the hyperbola model (8) and the average model (10) are compared. Fig. 7 shows the experimental results. The scenario is composed of monotonic increase/decrease and constant input. The responses for each model are shown in the figure. It is clear that the proposed hysteresis model is more accurate than the average model since the average model has offset error for all regions. In particular, when the input stops while increasing or decreasing, the output value is calculated to reflect the previous state. The results around 12.5 s and 22.5 shows that the hysteresis model generates ascending/descending curve values for increased/decreased inputs and stays after it, respectively. In addition, the experimental response indicates the value between ascending/descending curves when the sign of the input gradient changes rapidly, as shown at around 25 s. It can be confirmed that the proposed model reflects these physical phenomena and generates more accurate results than the average model with small error (RMSE of hyperbola model = 0.207 bar, RMSE of average model = 0.404 bar). The large

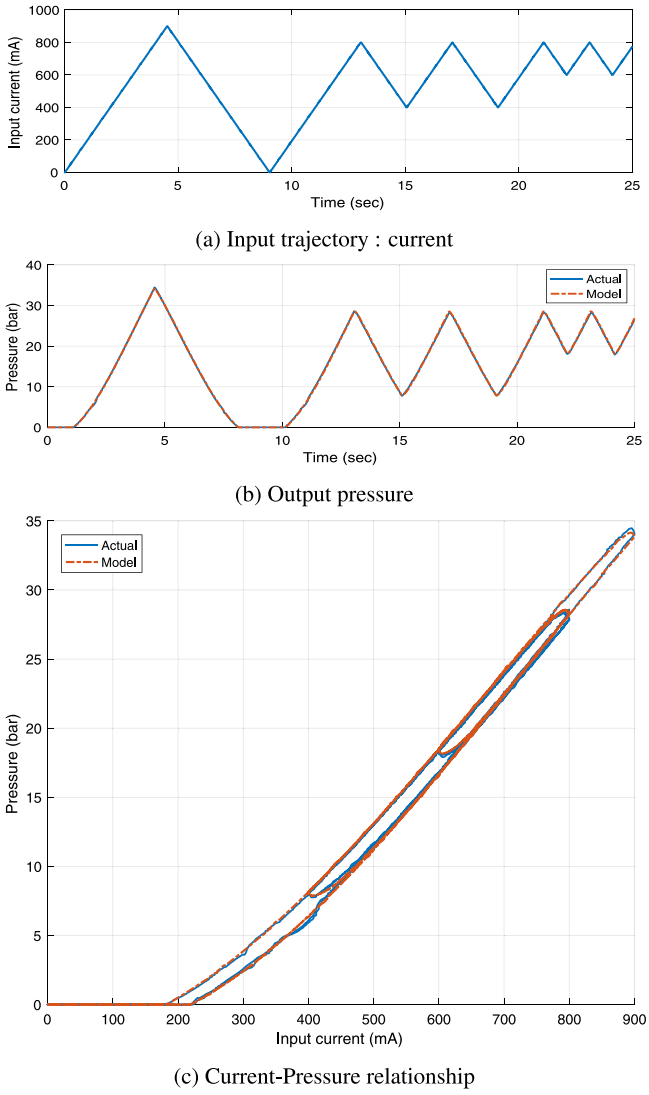

(a) Input trajectory : current

(b) Output pressure

(c) Current-Pressure relationship

Fig. 5. Model validation: comparison between actual and model value.

error around 24.7 s is caused by clutch dumping phase, which is not considered in this paper.

Model verification using driving data of production vehicles was also conducted. The current–pressure data from the Transmission Control Unit (TCU) were used to generate and compare the model response. These data contain an engaging–disengaging process of the clutch in shifting situations. Figs. 6a and 6b demonstrate the clutch pressure when clutch is in engaging/disengaging process, respectively. It is shown that the pressure profile forms very fast and dynamically during actual vehicle driving. As can be seen in the error plots, the proposed hysteresis model generated more accurate results than the average model for both cases. Except for errors generated by the filling process of the clutch chamber, the proposed hysteresis model produces actual values with small error.

The proposed hysteresis model based on the hyperbolic function will be used in the hysteresis compensation scheme in Section 3.1.

3. Controller design

3.1. Feed-forward controller design

As mentioned in the previous section, hysteresis model-based feed-forward control is widely known as a way to compensate for hysteresis.

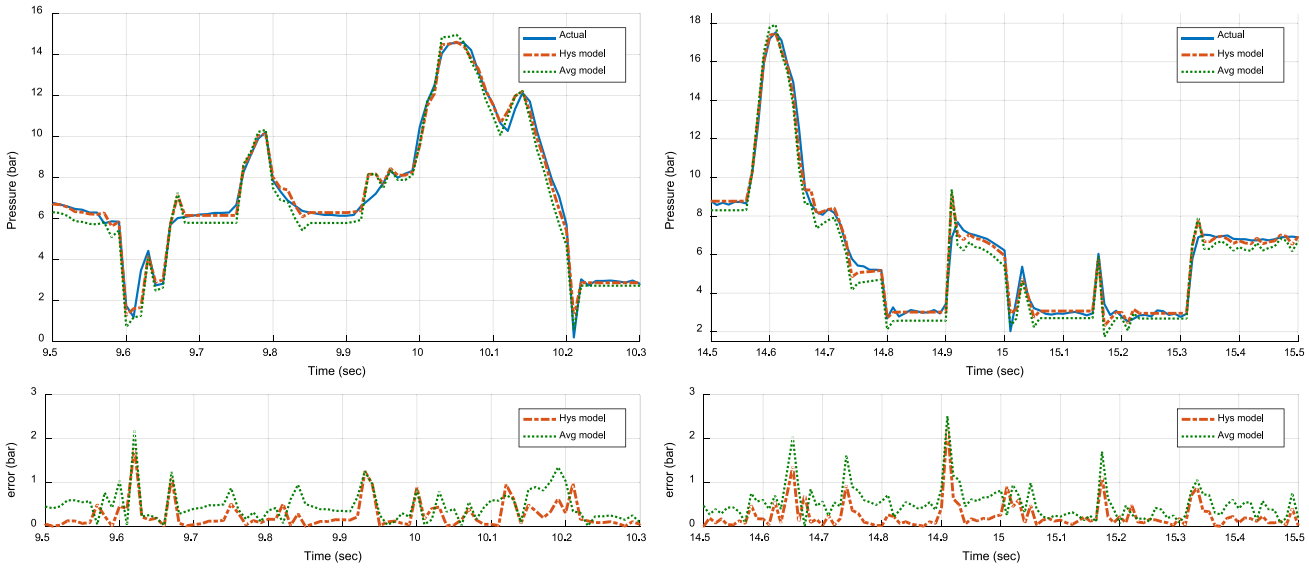

(a) On-comming clutch pressure trajectory

(b) Off-going clutch pressure trajectory

Fig. 6. Model validation through driving data.

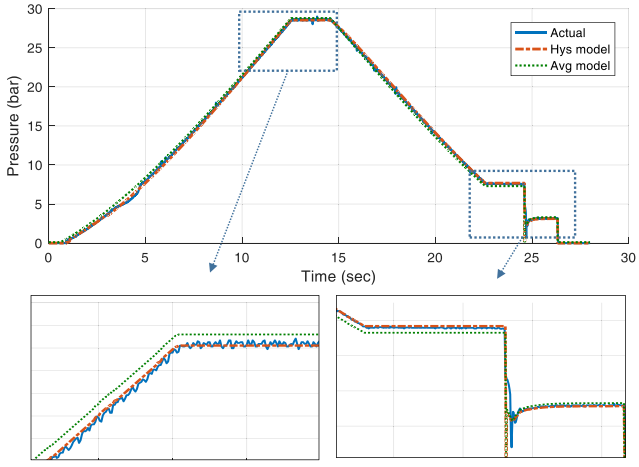

Fig. 7. Comparison between average model and proposed hysteresis model.

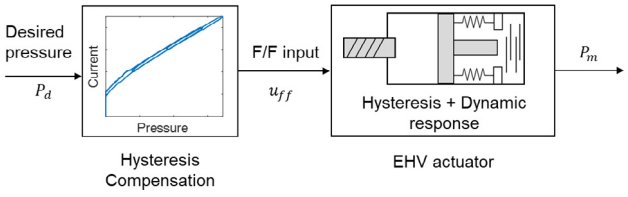

Fig. 8. Schematic of hysteresis model based feed-forward control.

The controller generates input commands using desired output values and forms an inverse of hysteresis model. The generated input command is applied to the control input of the plant. The inverse hysteresis model represents the pressure–current relationship, which is the axial transformation of Fig. 2. The overall scheme of the feed-forward controller using the inverse hysteresis model is described in Fig. 8.

The feed-forward control input should be calculated in real-time for use in on-line vehicle control. The inverse model of the proposed hysteresis model can be calculated analytically using (6). The hyperbolic model expressions in (6) and (8) were calculated to compute the output P_k according to the given input i_k. On the other hand, in order to calculate the feed-forward control input, the target input i_k for generating the desired pressure $P_{k,d}$ should be calculated. The results of the inverse model using (6) and (8) are described as follows:

$$i_k = f_{ref}^{-1}(P_{k,d} - \frac{a}{P_{k,d} - P_{t,k}}) = i_k(P_{k,d}; i_{k-1}, P_{k-1}) \tag{11}$$

The value of $P_{t,k}$ follows (7) because the previous step values (P_{k-1}, i_{k-1}) are all known. Therefore, the inverse hysteresis model shows the result of reflecting the previous step with only one tuning parameter, in the same way as in the proposed hysteresis model.

3.2. Feedback controller design

Feed-forward control has the advantage of fast response regardless of sensor information, but it has a disadvantage in that it is heavily influenced by model accuracy. Feed-forward control based on the hysteresis model proposed in the previous section determines the control performance according to the accuracy of the hysteresis model. In particular, the proposed model, (8), is strongly influenced by the accuracy of the reference curves (3), which indicate the steady-state characteristic. In an actual EHV system, reference curve changes slightly due to various factors such as fluid temperature, use time, amount of oil leakage, and so on. If only the feed-forward controller is applied, it is impossible to compensate for the influence of changes in the reference curve. Therefore, a feedback controller that can compensate for changes of plant characteristics is required.

However, as described in (1), a typical EHV is well known as a system with time delay. The time delay adversely affects the performance and stability of the feedback control and creates limitations in control (Nguyen, Ishihara, Krishnakumar, & Bakhtiari-Nejad, 2009). A Smith predictor or Proportional–Integral (PI) control is commonly used as a control method of time delay systems. In the case of EHV system and vehicle Controller Area Network (CAN) system, the time delay is not a fixed value but a value that varies with uncertainty. This feature makes it difficult to apply the conventional Smith Predictor to the target system. Thus, in this paper, in order to improve the applicability to production vehicles, a simple PI controller is used as feedback controller of the delayed system.

For the target EHV system, it is confirmed through various experimental data that the time delay of input to output is 10 ms to 30 ms. The stability is the biggest issue of feedback control of the

delayed system. Therefore, stability analysis was performed to design a stable PI controller for the target system. For the stability analysis, the current–pressure relationship was modeled as 1st order with time delay system (Thornton, Pietron, Yanakiev, McCallum, & Annaswamy, 2013). The transfer function of the plant is modeled as follows:

$$P(s) = \frac{k}{\tau s + 1} e^{-T_d s} \tag{12}$$

where T_d implies delayed time, k and τ is a model parameter that is determined based on experimental data. The parameters are set to $T_d = 0.04$, $k = 0.04$, and $\tau = 0.01$ for analysis. For convenience of analysis, the term $e^{-T_d s}$, which represents the time delay, is described in polynomial formula using Pade's 1st order approximation (Baker, Baker Jr, Baker JR, Graves-Morris, & Baker, 1996). By combining the approximation and (12), the plant model can be described as follows:

$$P(s) \approx \frac{k}{\tau s + 1} \cdot \frac{2 - T_d s}{2 + T_d s} \tag{13}$$

Pade's 1st order approximation describes the actual delay in the main control bandwidth well. As shown in (13), the plant is modeled as a system with the unstable zero. It can be inferred that large feedback gain can cause unstable closed-loop behavior due to the unstable zero. The PI controller proposed in this study has the following form:

$$C(s) = K_P + \frac{K_I}{s} \tag{14}$$

where K_P and K_I denote the proportional gain and the integral gain, respectively. A closed loop system representation can be constructed using the modeled plant and controller. The closed loop transfer function of (13) and (14) can be obtained as follows:

$$\begin{aligned} T(s) &= \frac{k(2 - T_d s)(K_P s + K_I)}{\tau T_d s^3 + (2\tau + T_d - kT_d K_P)s^2 + k(2 + 2kK_P - KT_d K_I)s + 2kK_I} \\ &\equiv \frac{k(2 - T_d s)(K_P s + K_I)}{a_0 s^3 + a_1 s^2 + a_2 s + a_3} \end{aligned} \tag{15}$$

For convenience of description, the polynomial coefficients of the denominator are expressed from high order to a_0 to a_3. Routh's stability criteria method is well known for evaluating the stability of a closed loop system (Morris, 2000). Based on Routh's stability criteria, the stability condition of (15) can be found as follows:

$$a_1 > 0 \tag{16}$$

$$a_1 a_2 - a_0 a_3 > 0 \tag{17}$$

The stability condition implies the condition and limitation of feedback gain that stabilizes the system. The condition for K_P can be obtained by (16), and the condition of K_I according to K_P can be obtained by (17). The feedback gain for system stability is calculated as follows:

$$\begin{aligned} &K_P < 35, \\ &K_I < 500 \quad \text{for max } K_P, \; K_I < 900 \quad \text{for min } K_P \end{aligned} \tag{18}$$

It can be confirmed that proportional control has strong limitations and most control should be applied based on integral control. In practice, a large proportional gain in the delay system causes instability. During slip control in the inertia phase, the target pressure contains high frequency component. In systems with input–output delay, the high frequency component further limits the feedback gain. Pade's approximation, used in the analysis, always represents less phase lag than the actual delay. This implies that the actual system has a stronger limitation than (18) according to the high frequency components. In the case of integral control, the margin is much larger than the proportional gain. However, this method has the disadvantage of slow response due to phase lag of the controller itself. Thus, sufficient tracking performance cannot be obtained by integral control alone. Consequently, (18) implies that feedback control alone cannot achieve desired tracking control performance. Therefore, in this paper, a controller that applies feed-forward and feedback control input simultaneously is proposed. The feed-forward controller uses the hysteresis model-based controller designed in the previous section. This is based on a very precise model, one that guarantees overall tracking performance. Considering the delay of the system, the feedback controller uses the PI controller within the stable margin. The integral controller plays a major role in compensating for control errors due to model uncertainty consisting of low frequency components.

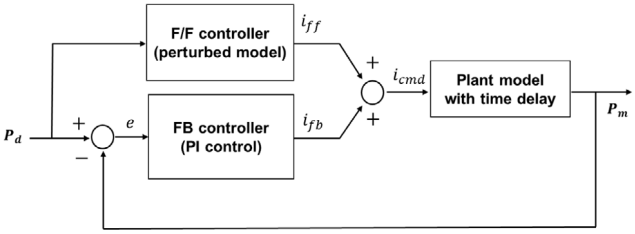

Fig. 9. Block diagram of the proposed hysteresis compensation control.

Simulation was conducted to verify the role and performance of the feedback controller. The simulation was constructed based on target pressure obtained during driving test of real vehicle. The plant was described as having a 30 ms time delay system using the current–pressure relationship and the hysteresis model of the actual vehicle. The controller applies feed-forward and feedback control at the same time, and the feed-forward controller adopts the controller design in Section 3.1. In constructing the feed-forward scheme, the I–P reference curve is distinguished from the plant by adding an error to the true value. The added error reflects the model error due to oil temperature changes. The PI controller was designed as a feedback controller. The control sampling frequency was 100 Hz; an overall schematic of the simulation is provided in Fig. 9. In the simulation, feedback gain is set to $K_P = 1$ and $K_I = 5$.

The simulation results are described in Fig. 10. Figs. 10a and 10b compare the absence and presence of the feedback controller. Fig. 10a shows the result when only feed-forward control is applied. Since there exist a difference between the model used in the plant and feed-forward controller, the output pressure follows the desired input trend, but a steady-state offset error occurs. Fig. 10b shows the control results when additional feedback control is applied. It can be confirmed that the offset error appearing from feed-forward control is compensated for by feedback control.

Figs. 10c and 10d describe each control input when feed-forward and feedback are simultaneously applied. The magnitude of the feed-forward and feedback control inputs applied to the plant are compared in Fig. 10c. As shown in the graph, the feed-forward input is much more dominant than feedback input. The generated feed-forward input reflects the tendency of the desired pressure. Thus, most tracking performance can be guaranteed with feed-forward input. Fig. 10d shows a comparison between control input generated by proportional control and integral control. Obviously, proportional control contains many high frequency components, which can cause instability in a delayed system. As with the stability analysis results, it is confirmed that proportional control alone cannot generate stable control inputs. On the other hand, in the case of the integral control, the integrator itself suppresses the high frequency component and compensates for the steady-state offset error in the low frequency region. Therefore, if both feed-forward and feedback control are used simultaneously, each controller can perform its role and expect good tracking performance. In conclusion, a combined controller, hysteresis model-based feed-forward controller, and Proportional–Integral feedback controller is proposed as a pressure tracking controller for EHV system.

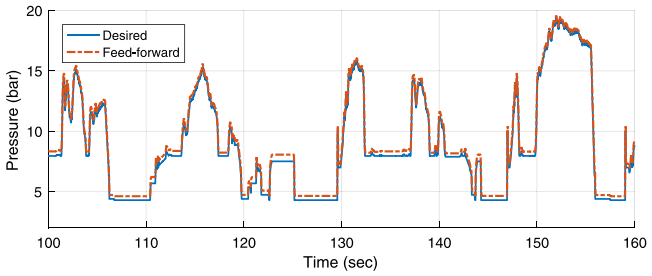

(a) Result of feed-forward control

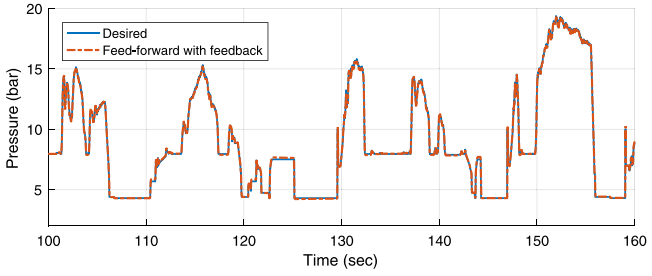

(b) Result of feedback control with feed-forward control

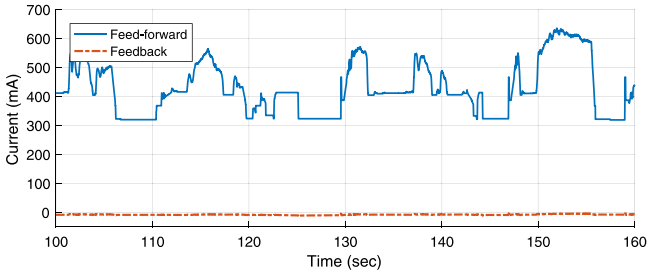

(c) Comparison betweeen feed-forward and feedback input

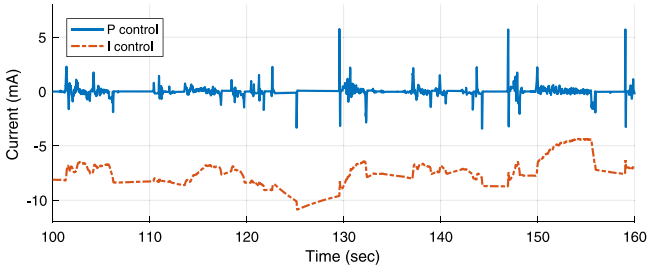

(d) Comparison betweeen P and I control input

Fig. 10. Simulation results: validation of feedback control.

4. Experimental results

4.1. Experiment overview

In order to verify the performance of the proposed pressure controller, experiments were conducted on an EHV equipped in a production vehicle. The target vehicle is a vehicle equipped with a wet DCT based on a hydraulic actuator. A pressure sensor is installed to measure the pressure in each clutch chamber and the control input is applied by the current command to the solenoid valve. The actual current follows the command value through the internal control logic. In this paper, it is assumed that the current control is sufficiently faster than the other control logics. The proposed control logic is directly embedded in the TCU and data transmission and reception is performed using vehicle CAN network. The sampling frequency of data logging and control logic are fixed at 100 Hz.

Fig. 11. Experimental production vehicle (Hyundai motors, 0000).

Several experiments were conducted to validate the performance of the proposed pressure controller. The purpose of the experiment was to verify the control performance of the feed-forward controller based on the hysteresis model and the feedback controller. In order to verify the performance of each controller, a case in which only feed-forward control is applied and a case in which feedback control is added were analyzed separately. The experimental scenario was to track the profiles of the clutch pressure generated during normal driving. The driving test included all stages of gear shift, torque phase, inertia phase, and slip control command. The pressure profile is generated from the upper controller of the TCU; this process is not included in this paper. This paper deals with the tracking control performance of the generated pressure profile. The target system is a system with time delay, as shown in Eq. (1). Obviously, the best control output of a time delay system with an indeterministic input is an output that tracks a reference profile with a delayed time. Thus, the control performance was analyzed by comparing the measured pressure and the delayed reference profile (see Fig. 11).

4.2. Feed-forward control based on hysteresis model

As mentioned in Section 2, the purpose of the hysteresis model is to accurately describe the behavior of the plant and generate a current input value for the target pressure. The feed-forward controller, based on the hysteresis model, was applied to the TCU for clutch pressure control. The experimental results for clutch 1 are depicted in Fig. 12a. It can be seen that the feed-forward controller obtains good tracking performance for the overall region. RMSE of the experiment is 0.436bar for an 800 s driving scenario. This RMSE is slightly larger than the model error shown in Section 2 because the actual system has uncertainty. This causes small steady-state error for a certain pressure range.

Feed-forward control has the advantage of fast and agile response. In order to verify the tracking performance of the proposed model for fast input, a test was conducted that included a tip-in/tip-out scenario. The test results are depicted in Figs. 12b to 12d. The figures show throttle pedal position and pressure profile of clutch 1 and clutch 2, which represent driving conditions. The pressure profile due to the tip-in/tip-out behavior appears at 10.5 to 11.5 s. It can be seen that a high frequency pressure profile is generated in clutch 2 due to the fast input. Despite the high frequency profile, the proposed feed-forward controller based on the hysteresis model follows the target pressure accurately without lag or delay. Thus, it can be confirmed that the controller performs well in overall tracking for the dynamic input profile even if some error occurs due to the uncertainty of the model.

4.3. Feed-forward control with feedback control

The feed-forward control shown in the previous section has been proved to provide fast and accurate control performance when the reference model is correct. However, in actual driving situations, the reference model can change slightly due to change of fluid temperature,

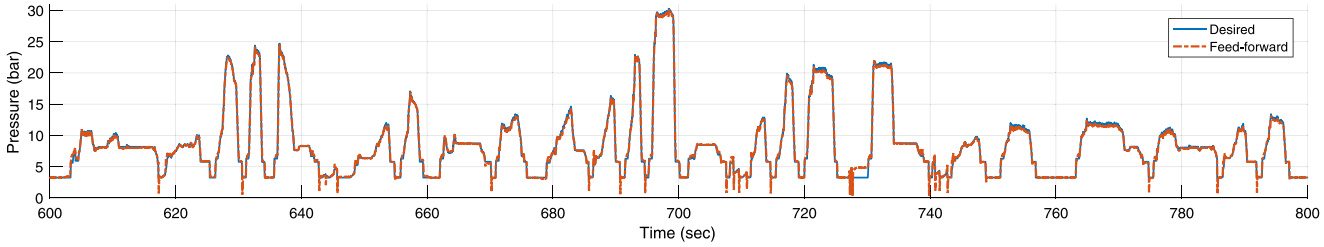

(a) Result of feed-forward control

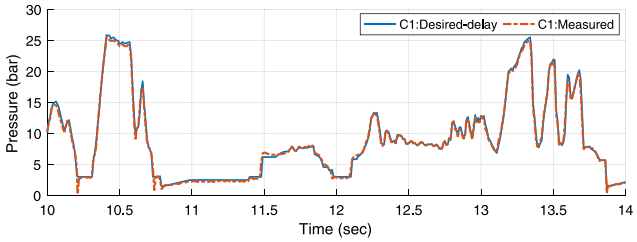

(b) Feed-forward control : clutch 1

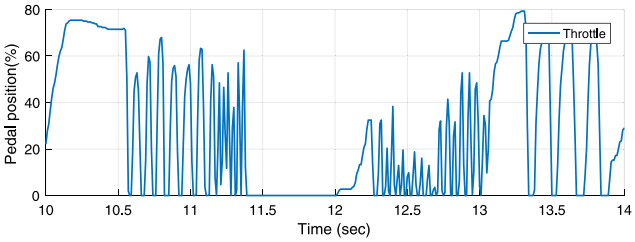

(c) Accel pedal position : Tip in/out behavior

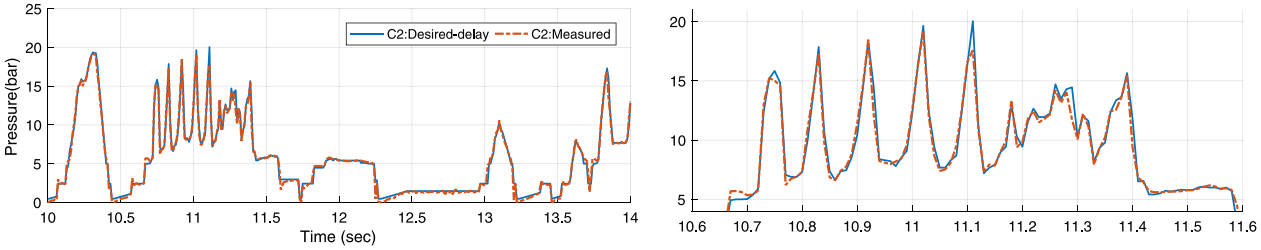

(d) Feed-forward control : clutch 2 - Tip in/out behavior

Fig. 12. Experiment results: Feed-forward control based on hysteresis model.

Table 1
RMSE of experimental results: various feedback gain.

RMSE(bar)	Clutch 1	Clutch 2
Feed-forward only	0.413	0.487
Feedback with $K_P = 1,\ K_I = 5$	0.352	0.362
Feedback with $K_P = 1,\ K_I = 10$	0.312	0.345

air gap, and aging problems. These factors can cause a steady-state error that cannot be solved only by feed-forward control. The tendency of the input profile, such as ascending and descending, can be described by the feed-forward control, but errors due to other model uncertainties must be compensated for through feedback control. The feedback controller designed in Section 3.2 is added to the feed-forward controller applied in Section 3.1 above. In experiments, the feedback control was applied after the filling phase had ended (over 6bar), in order to exclude the influence of the control result of filling phase; this is not covered in this paper.

Fig. 13 shows experimental results comparing the feedback control according to the various feedback gains. The results with only feed-forward control (Fig. 13a), feedback with $K_P = 1,\ K_I = 5$ (Fig. 13b), and feedback with $K_P = 1,\ K_I = 10$ (Fig. 13c) were used for the comparison group. The same feed-forward controller and test driving cycle were used for all experiments. The control performance is validated by not only RMSE of the overall driving cycle, but also by comparison of performance for specified pressure ranges. The normal driving test has the disadvantage that it is difficult to generate the same profile under the same conditions for each experiment. Thus, the control performance according to the change of feedback gain was analyzed by comparing the pressure profile generated under rapid acceleration condition. The specified pressure range of the rapid acceleration scenario is 20 to 26bar. In results for feed-forward control, there exists steady-state offset error due to model uncertainties. However, experimental results in Fig. 13c shows no offset error due to feedback control input, which means better tracking performance than when only feed-forward control is applied. Comparing the control results at 20 to 26bar, it can be seen that the feedback control more actively compensates for feed-forward error as the gain increases. Also, RMSE values of the overall driving test with various gain values are summarized in Table 1. It can be confirmed that feedback control enhances the control performance by compensating for model error.

Figs. 13d and 13e show the feed-forward and feedback control input from Fig. 13c. Similar to the simulation analysis in Section 3, it can be seen that the feed-forward inputs are much more dominant; however, feedback control is used to compensate for errors due to model uncertainty. The feedback control input value depends on the accuracy of the model. The feedback input increases as the model becomes more inaccurate. Therefore, it can be concluded that an appropriate gain value can compensate for the uncertainty of the model and enhance the control performance.

Consequently, feed-forward control based on the hysteresis model proposed in Section 2, and the feedback control designed in Section 3 show good tracking performance for EHV. As described in Section 2, the proposed controller is based on a predefined reference curve. Once the reference curve is defined, there is an advantage that tracking performance can be guaranteed without additional parameter maps or rule-based control of reference curve value, which changes due to various factors in actual vehicles. Also, because of the small number of tuning parameters, it is expected that control system will be easy to apply to production vehicles and will improve the control performance of the overall shift process.

5. Conclusion

This study proposes a new pressure control logic for a hydraulic actuator used in vehicle transmission systems. The proposed controller

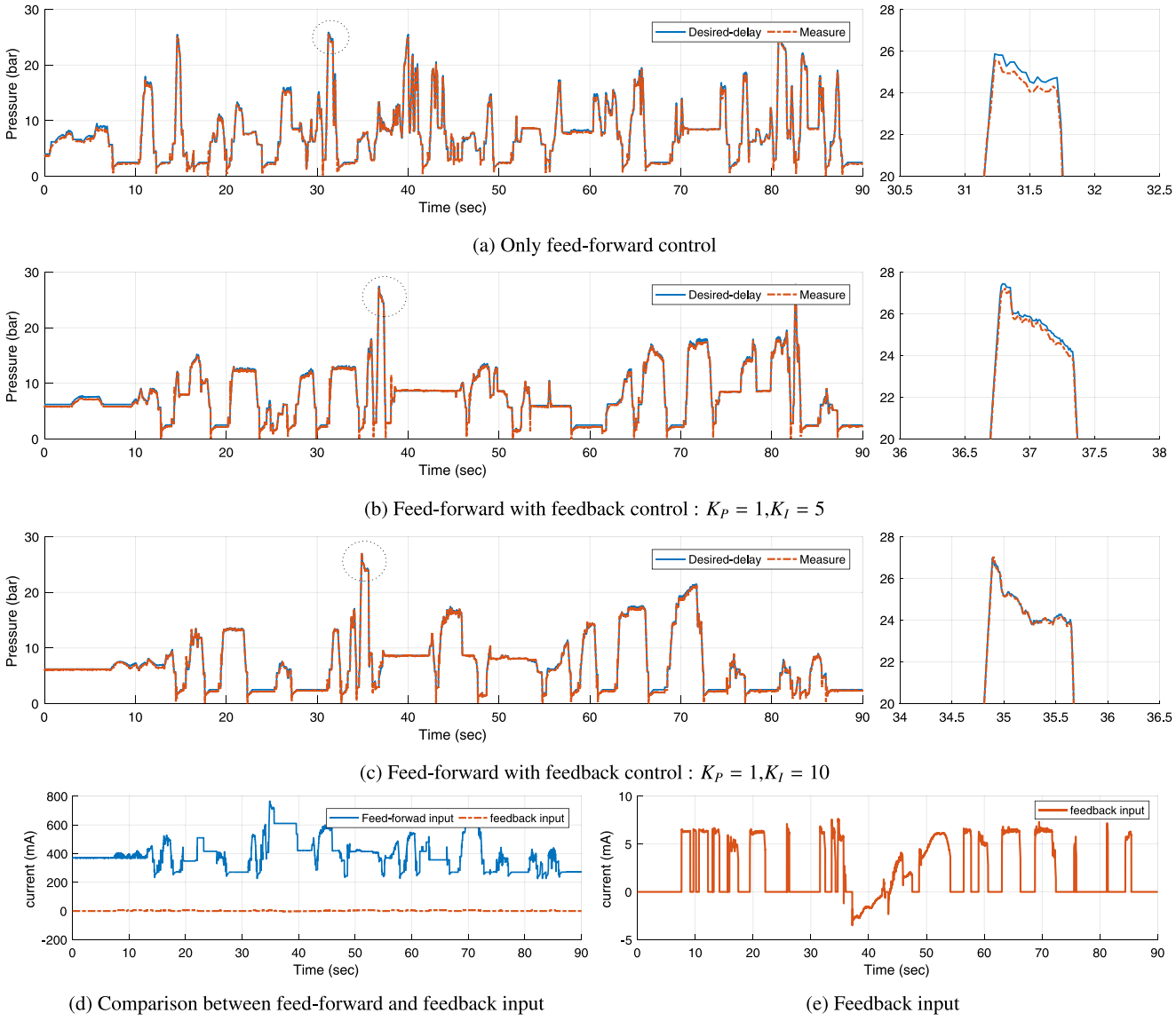

(a) Only feed-forward control

(b) Feed-forward with feedback control : $K_P = 1, K_I = 5$

(c) Feed-forward with feedback control : $K_P = 1, K_I = 10$

(d) Comparison between feed-forward and feedback input

(e) Feedback input

Fig. 13. Experiment results: Feed-forward control with feedback control.

consists of model-based feed-forward control considering the physical characteristics of hydraulic actuators and feedback control to cope with model error and uncertainty. A key contribution of this paper is the proposal of a new hysteresis model that reflects the physical phenomena and the designing of a pressure control logic based on the proposed model. The hysteresis model uses a continuous function to precisely describe the dynamic input. Using the model, a feed-forward input is generated, which enables fast and accurate tracking of the pressure profile generated during the shift control. Especially in the case of slip control during inertia phase of the shifting process, the pressure profile includes many high frequency components and chattering signals, but it is confirmed that the hysteresis model-based controller accurately describes all of them. The proposed model is expected to useful not only EHV system but also many systems with hysteresis. Moreover, feedback controller is added to feed-forward controller to compensate for model errors and uncertainties. The feedback controller is designed based on stability analysis of the time delay system, which is a characteristic of EHV system. The proposed controller is embedded into TCU of a production vehicle to verify its performance experimentally. Experimental results reveal that performance of the proposed controller is sufficient for it to be used in real car applications. Consequently, this study is expected to improve the control performance of hydraulic actuators, which is essential for the modern shifting control process. In particular, the simplicity of the logic and the small number of tuning parameters are expected to be convenient for vehicle applications.

Declaration of competing interest

The authors declare that they have no known competing financial interests or personal relationships that could have appeared to influence the work reported in this paper.

Acknowledgments

This research was supported by Hyundai Motor Company; in parts by the BK21+ program through the NRF funded by the Ministry of Education of Korea (No. 2017R1A2B4004116).

References

Al Janaideh, M., Rakheja, S., & Su, C.-Y. (2011). An analytical generalized prandtl–ishlinskii model inversion for hysteresis compensation in micropositioning control. *IEEE/ASME Transactions on Mechatronics*, *16*(4), 734–744.

Baker, G. A., Baker Jr, G. A., Baker JR, G. A., Graves-Morris, P., & Baker, S. S. (1996). *Padé approximants, Vol. 59*. Cambridge University Press.

Balau, A.-E., Caruntu, C.-F., & Lazar, C. (2011). Simulation and control of an electro-hydraulic actuated clutch. *Mechanical Systems and Signal Processing*, *25*(6), 1911–1922, Interdisciplinary Aspects of Vehicle Dynamics.

van Berkel, K., Hofman, T., Serrarens, A., & Steinbuch, M. (2014). Fast and smooth clutch engagement control for dual-clutch transmissions. *Control Engineering Practice*, *22*, 57–68.

Choi, W., Won, J., Lee, J., & Park, J. (2017). Low stiffness design and hysteresis compensation torque control of sea for active exercise rehabilitation robots. *Autonomous Robots*, *41*(5), 1221–1242.

Choudhury, M. S., Thornhill, N. F., & Shah, S. L. (2005). Modelling valve stiction. *Control Engineering Practice*, *13*(5), 641–658.

Eielsen, A. A., Gravdahl, J. T., & Pettersen, K. Y. (2012). Adaptive feed-forward hysteresis compensation for piezoelectric actuators. *The Review of Scientific Instruments*, *83*(8), 085001.

Fu, Y., Liu, Y., Cui, L., & Xu, X. (2016). Dynamic analysis and control strategy of wet clutches during torque phase of gear shift. *Journal of Mechanical Science and Technology*, *30*(4), 1479–1496.

Galvagno, E., Velardocchia, M., & Vigliani, A. (2011). Dynamic and kinematic model of a dual clutch transmission. *Mechanism and Machine Theory*, *46*(6), 794–805.

Glielmo, L., Iannelli, L., Vacca, V., & Vasca, F. (2006). Gearshift control for automated manual transmissions. *IEEE/ASME Transactions on Mechatronics*, *11*(1), 17–26.

Guo, W., Liu, Y., Zhang, J., & Xu, X. (2014). Dynamic analysis and control of the clutch filling process in clutch-to-clutch transmissions. *Mathematical Problems in Engineering*, *2014*.

(0000). Hyundai motors, https://www.hyundai.com/.

Kim, S., Oh, J., & Choi, S. (2017). Gear shift control of a dual-clutch transmission using optimal control allocation. *Mechanism and Machine Theory*, *113*, 109–125.

Kim, S., Oh, J. J., & Choi, S. B. (2018). Driveline torque estimations for a ground vehicle with dual-clutch transmission. *IEEE Transactions on Vehicular Technology*, *67*(3), 1977–1989.

Kulkarni, M., Shim, T., & Zhang, Y. (2007). Shift dynamics and control of dual-clutch transmissions. *Mechanism and Machine Theory*, *42*(2), 168–182.

Montanari, M., Ronchi, F., Rossi, C., Tilli, A., & Tonielli, A. (2004). Control and performance evaluation of a clutch servo system with hydraulic actuation. *Control Engineering Practice*, *12*(11), 1369–1379.

Morris, K. A. (2000). *Introduction to feedback control*. Academic Press, Inc..

Naser, M. F. M., & Ikhouane, F. (2015). Hysteresis loop of the lugre model. *Automatica*, *59*, 48–53.

Nguyen, N., Ishihara, A., Krishnakumar, K., & Bakhtiari-Nejad, M. (2009). Bounded linear stability analysis-a time delay margin estimation approach for adaptive control. In *AIAA guidance, navigation, and control conference* (p. 5968).

Oh, J. J., & Choi, S. B. (2015). Real-time estimation of transmitted torque on each clutch for ground vehicles with dual clutch transmission. *IEEE/ASME Transactions on Mechatronics*, *20*(1), 24–36.

Ru, C., Chen, L., Shao, B., Rong, W., & Sun, L. (2009). A hysteresis compensation method of piezoelectric actuator: Model, identification and control. *Control Engineering Practice*, *17*(9), 1107–1114.

Ryba, Ł., Dokoupil, J., Voda, A., & Besançon, G. (2017). Adaptive hysteresis compensation on an experimental nanopositioning platform. *International Journal of Control*, *90*(4), 765–778.

Sheng, C., Hai, N. L., Cheng, Y. X., & Bao-Lin, T. P. (2013). Proportional solenoid valve flow hysteresis modeling based on pso algorithm. In *Instrumentation, measurement, computer, communication and control (IMCCC), 2013 third international conference on* (pp. 1064–1067). IEEE.

Song, X., Zulkefli, M. A. M., & Sun, Z. (2010). Automotive transmission clutch fill optimal control: An experimental investigation. In *American control conference (ACC), 2010* (pp. 2748–2753). IEEE.

Thornton, S., Pietron, G. M., Yanakiev, D., McCallum, J., & Annaswamy, A. (2013). Hydraulic clutch modeling for automotive control. In *52nd IEEE conference on decision and control* (pp. 2828–2833). IEEE.

Vasca, F., Iannelli, L., Senatore, A., & Reale, G. (2011). Torque transmissibility assessment for automotive dry-clutch engagement. *IEEE/ASME Transactions on Mechatronics*, *16*(3), 564–573.

Walker, P. D., Zhang, N., & Tamba, R. (2011). Control of gear shifts in dual clutch transmission powertrains. *Mechanical Systems and Signal Processing*, *25*(6), 1923–1936, Interdisciplinary Aspects of Vehicle Dynamics.

Walker, P. D., Zhu, B., & Zhang, N. (2014). Nonlinear modeling and analysis of direct acting solenoid valves for clutch control. *Journal of dynamic systems, measurement, and control*, *136*(5), 051023.

Xu, Q., & Li, Y. (2010). Dahl model-based hysteresis compensation and precise positioning control of an XY parallel micromanipulator with piezoelectric actuation. *Journal of dynamic systems, measurement, and control*, *132*(4), 041011.